Theabrownin inhibits the cytoskeleton-dependent cell cycle, migration and invasion of human osteosarcoma cells through NF-κB pathway-related mechanisms

WANGDONG JIN[1], CHAOQUN GU[1], LI ZHOU[2], XINYU YANG[2], MENGYUAN GUI[2], JIN ZHANG[3], JIE CHEN[1], XIAOQIAO DONG[4], QIANG YUAN[1] and LETIAN SHAN[2]

[1]College of Pharmacy, and [2]The First Affiliated Hospital, Zhejiang Chinese Medical University, Hangzhou, Zhejiang 310053; [3]Theabio Co., Ltd., Hangzhou, Zhejiang 311121; [4]Department of Neurosurgery, Affiliated Hangzhou First People's Hospital, Zhejiang University School of Medicine, Hangzhou, Zhejiang 310006, P.R. China

Received March 6, 2020; Accepted August 18, 2020

DOI: 10.3892/or.2020.7801

Abstract. Considering the high metastatic potential of osteosarcoma, not only pro-apoptosis, but also anti-metastasis is important for anti-osteosarcoma therapy. Previously, the authors reported the pro-apoptotic and tumor-inhibitory effects of theabrownin (TB) on osteosarcoma cells; however, its effects on the metastasis-related migration and invasion of osteosarcoma cells remain unknown. The present study conducted RNA sequencing (RNA-seq) on xenograft zebrafish samples and performed *in vitro* experiments, including RT-qPCR, cell viability analysis, clone formation assay, cell cycle analysis, immunofluorescence, cell migration assay, cell invasion assay, wound healing assay and western blot (WB) analysis to evaluate the anti-metastatic effects and mechanism of TB against osteosarcoma cells. The RNA-seq data revealed that TB significantly downregulated the expression of genes involved in the microtubule bundle formation of U2OS cells, which was verified by RT-qPCR. The cell viability and clone formation data indicated that TB significantly inhibited U2OS cell viability and colony numbers. The results of cell cycle analysis revealed the blocked cell cycle progression of U2OS by TB. The immunofluorescent data revealed an evident cytoskeleton-inhibitory effect of TB against the microfilament and microtubule formation of U2OS cells. The results of cell migration and invasion demonstrated that TB significantly inhibited U2OS cell migration and invasion. The results of WB analysis revealed that TB significantly regulated key molecules of epithelial-mesenchymal transition [EMT; e.g., E-cadherin, vimentin, Snail-1, Slug and zinc finger E-box-binding homeobox 1 (ZEB-1)] and those of the nuclear factor (NF)-κB pathway (e.g., NF-κB, phospho-IKKα and phospho-IKKβ), indicating that NF-κB pathway-related EMT suppression may mediate the mechanisms underlying the anti-migratory and anti-invasive effects of TB against osteosarcoma. To the best of our knowledge, this is the first study on the inhibitory effects and mechanisms of TB on the cytoskeleton-dependent cell cycle, migration and invasion of human osteosarcoma cells. The findings presented herein suggest that TB may be a promising anti-metastatic candidate for anti-osteosarcoma therapy.

Correspondence to: Professor Letian Shan, The First Affiliated Hospital, Zhejiang Chinese Medical University, 548 Binwen Road, Binjiang, Hangzhou, Zhejiang 310053, P.R. China
E-mail: letian.shan@zcmu.edu.cn

Professor Qiang Yuan, College of Pharmacy, Zhejiang Chinese Medical University, 548 Binwen Road, Binjiang, Hangzhou, Zhejiang 310053, P.R. China
E-mail: yuanqiang0825@sina.com

Abbreviations: TB, theabrowin; RNA-seq, RNA sequencing; RT-qPCR, reverse transcription-quantitative PCR; EMT, epithelial-mesenchymal transition; p-IKKα, phospho-IKKα; p-IKKβ, phospho-IKKβ; BMSCs, bone marrow-derived mesenchymal stem cells; p-IκBα, phospho-IκBα; FBS, fetal bovine serum; PBS, phosphate-buffered saline; CCK-8, Cell Counting Kit-8; BSA, bovine serum albumin; OD, optical density; TBST, tris-buffered saline-Tween-20

Key words: theabrownin, osteosarcoma, U2OS cells, cell migration, cell invasion, epithelial-mesenchymal transition, nuclear factor-κB

Introduction

Osteosarcoma is the most common malignant bone tumor affecting children and adolescents worldwide, and it has features of local aggressive growth and a high metastatic potential (1). It occurs more frequently in males than in females with an incidence ratio of 1.43:1 (2,3). The metaphysis of the lower long bones is typically the primary site of osteosarcoma, and metastases are present in approximately 20% of cases (4,5). Distant metastases of osteosarcoma, such as lung metastases, are difficult to control and usually have a poor prognosis (6). The etiology of osteosarcoma is complex and linearly associated with increasing doses of radiation (7). Certain rare heritable cancer predisposition syndromes are also associated with an increased risk of osteosarcoma (8). The majority of patients with osteosarcoma suffer pain in the affected region,

partially from localized swelling, motion limitation and pathological fractures (4,9). Currently, chemotherapeutic agents, such as cisplatin, methotrexate, doxorubicin, etoposide and ifosfamide, are usually administered before or after surgery to prevent the tumor from spreading throughout the body (5,10). However, their outcomes are not satisfactory and the 5-year overall survival rate of affecting patients is estimated at approximately 25% (11). Patients with distant metastases have a poorer prognosis, with a 5-year survival rate of only 20% (6). Therefore, novel treatment strategies are urgently required to improve the outcome and quality of life of patients with osteosarcoma.

Tea has a history with dates back centuries, and has become the most popular beverage in Asia, particularly in China. By using fresh or fermented leaves of *Camellia sinensis* O. Kuntze, tea drinks have unique flavors and potential health benefits, such as anti-fatigue, anti-hyperlipidemia, and anti-hypercholesterolemia activities (12-14). Epidemiological surveys showed that consuming more than 10 cups of tea per day could prevent cancer occurrence, indicating the anti-cancer potential of tea (15,16). As a representative bioactive component of tea, theabrownin (TB) has been reported to possess anticancer activity against lung carcinoma and osteosarcoma in previous studies by the authors (17,18). TB is a reddish-brown pigment derived from polyphenol components by oxidation, and it has the advantages of high water-solubility and low toxicity over other pigments. The authors have previously demonstrated that TB exerts potent pro-apoptotic effects against U2OS osteosarcoma cells by triggering DNA damage through the p53 signaling pathway, whereas it exhibited no toxicity on normal tissue *in vivo* or on normal cells [bone marrow-derived mesenchymal stem cells (BMSCs)] (17). These findings indicate that TB may be a promising candidate for osteosarcoma therapy.

Considering that both U2OS cells and BMSCs are p53 wild-type cells, the activation of the p53 signaling pathway may not be the only mechanism of TB, since it cannot explain the diverse effectiveness of TB on U2OS cells and normal cells. Therefore, it was hypothesized that TB may have other mechanisms of action in addition to its p53-mediated mechanisms. To examine this hypothesis, the present study employed xenograft zebrafish samples to conduct RNA sequencing and performed molecular experiments for further verification and investigation. To date, only the p53-mediated mechanism has been reported to be associated with the anticancer effects of TB. Thus, the present study presents a novel report on the anti-osteosarcoma mechanisms of TB.

Materials and methods

Chemicals and reagents. TB (>90% purity) was purchased from Theabio Co., Ltd. Fetal bovine serum (FBS) was purchased from CellMax. Phosphate-buffered saline (PBS) and McCoy's 5A medium were purchased from Gibco; Thermo Fisher Scientific, Inc. CCK-8, phosphatase inhibitor cocktail, All-in-One cDNA Synthesis SuperMix and 2X SYBR-Green qPCR Master Mix were purchased from Bimake. RNAiso Plus was purchased from Takara Biotechnology Co., Ltd. Crystal violet (0.1%) was purchased from Sigma-Aldrich; Merck KGaA. Nocodazole was purchased from Selleck Chemicals. Propidium iodide/RNase staining buffer was purchased from BD Biosciences. Acti-stain™ 535 phalloidins (cat. no. PHDR1) was purchased from Cytoskeleton, Inc. Tris-buffered saline, Tween-20, Triton X-100, paraformaldehyde and bovine serum albumin (BSA) were purchased from Sangon Biotechnology, Inc. ProLong Diamond Antifade Mountant with DAPI, the Pierce BCA protein assay kit and RIPA lysis buffer were purchased from Thermo Fisher Scientific, Inc. Polyvinylidene fluoride membranes and Immobilon Western Chemiluminescent HRP substrate were purchased from Merck KGaA. Proteinase inhibitor cocktail was purchased from Roche Diagnostics. Transwell chamber systems and Matrigel were purchased from Corning, Inc. Recombinant human TNF-α (cat. no. 300-01A) was purchased from PeproTech Inc. Anti-tubulin antibody-microtubule marker (cat. no. ab195883) was purchased from Abcam. β-actin (cat. no. A3854) was purchased from Sigma Chemical Co. All the primary antibodies (Vimentin (cat. no. 5741), Slug (cat. no. 9585), Snail (cat. no. 3879), Claudin-1 (cat. no. 13255), ZEB1 (cat. no. 3396), E-Cadherin (cat. no. 3195), N-Cadherin (cat. no. 13116), IKKα (cat. no. 11930), IKKβ (cat. no. 8943), IκBα (cat. no. 4814), NF-κB (cat. no. 8242), phospho-IKKα/β (Ser176/180) (cat. no. 2697), phospho-IκBα (Ser32) (cat. no. 2859), Histone-H3 (cat. no. 4499) used for western blot analysis were purchased from Cell Signaling Technology, Inc. Fluorescein (FITC)-conjugated AffiniPure Donkey Anti-Rabbit IgG (H+L) (cat. no. 711-095-152) and Peroxidase AffiniPure Goat Anti-Mouse IgG (H+L) (cat. no. 115-035-062) was purchased from Jackson ImmunoResearch Laboratories, Inc.

Xenograft experiment and RNA sequencing (RNA-seq). The xenograft experiment on larval zebrafishes was conducted in a previous study by the authors (17). Briefly, a xenograft model of osteosarcoma was established by the microinjection of U2OS cells to larval zebrafishes at the age of 3 days followed by the orally administration of TB at 2.13 to 21.3 μg/ml. Following 24 h of treatment, all fish at the age of <5 days were anesthetized by freezing at 0˚C for 10 min to observed and detect tumor growth, followed by sacrificing using liquid nitrogen. The whole larval zebrafishes were used for RNA extraction as follows: i) The fish bodies in each group [model group and TB-treated group (2.13 μg/ml)] were collected into an Eppendorf tube and mixed with 0.5 ml of TRIzol reagent for cell lysis; ii) the mixture was homogenized and supplemented with 0.5 ml chloroform, followed by centrifugation at 12,000 x g for 10 min at 4˚C to separate the RNA and protein; and iii) the separated aqueous phase was collected and supplemented with the same amount of isopropanol, followed by centrifugation at 12,000 x g for 10 min at 4˚C to deposit the RNA. The concentration of total RNA was quantified using a NanoDrop 2000 spectrophotometer (Thermo Fisher Scientific, Inc.). For cDNA library preparation, 3 μg total RNA was captured by Dynabeads Oligo (Life Technologies; Thermo Fisher Scientific, Inc.) and sheared to fragments of ~200 bp. Reverse transcription was performed using the Superscript III cDNA Synthesis Kit (Life Technologies; Thermo Fisher Scientific, Inc.). The cDNA was end-repaired, A-tailed and ligated to Illumina sequencing adapters and amplified by PCR. Library preparation was performed using the TruSeq RNA LT V2 Sample Prep Kit (Illumina). Sequencing was performed on the Illumina XTen Sequencing System (Illumina). The raw

Table I. Primer sequences used for RT-qPCR.

Gene	Forward primer	Reverse primer
ACTIN	5'-ATAGCACAGCCTGGATAGCAACGTAC-3'	5'-CACCTTCTACAATGAGCTGCGTGTG-3'
MYH2	5'-CTGAGGGAGGAGCGACTCT-3'	5'-CTCGGGCTTATACACAGGCA-3'
MYH7	5'-ACTGCCGAGACCGAGTATG-3'	5'-GCGATCCTTGAGGTTGTAGAGC-3'
TUBA1B	5'-GTACCGTGGTGACGTGGTTC-3'	5'-CTTGGCATACATCAGGTCAA-3'
TUBB2B	5'-ATCAGCAAGATCCGGGAAGAG-3'	5'-CCGTGTCTGACACCTTGGGT-3'

reads were processed by removing the adaptors, sequences with uncertain bases, low-quality sequence, and sequences of <50 bp to generate clean reads. The clean reads from the Fastq files were mapped to human reference genome using Spliced Transcripts Alignment to Reference (STAR) software (version 2.7.1a). Differential expression analysis of the different groups was performed with biological replicates using DESeq software (version 1.30.0). A P-value of 0.05 was set as the threshold for significant differential expression.

Cell line and culture. The human osteosarcoma cell line, U2OS, without mycoplasma infection was identified and provided from Shanghai Cell Bank of Chinese Academy of Sciences. The cells were cultured in McCoy's 5A medium containing 10% FBS at 37˚C in humidified atmosphere containing 5% CO_2. The medium was changed daily and the cells at logarithmic growth phase were prepared for the subsequent experiments.

Reverse transcription-quantitative PCR (RT-qPCR). For verifying the results of RNA sequencing, qPCR assay was performed. Total RNA was extracted from the U2OS cells with and without TB treatment using RNAiso Plus (Takara Biotechnology Co., Ltd.), followed by cDNA synthesis using an All-in-One cDNA Synthesis SuperMix. Subsequently, the 2X SYBR-Green qPCR Master Mix kit was used for transcript quantification with specific primers. All the reactions were set up according to the manufacturer's instructions. At the end of each reaction, a melting curve analysis was performed. Data were normalized to the expression of ACTIN and presented using the $2^{-\Delta\Delta Cq}$ method (Table I) (19).

Cell viability assay. The viability of the U2OS cells was determined by CCK-8 assay. The cells were seeded on 96-well plates at a density of $1x10^4$ cells/well in 200 μl McCoy's 5A medium contained 10% FBS. Following adherence for 24 h, the cells were respectively treated with TB at 0, 10, 20, 30, 40, 50, 60, 70, 80, 90 and 100 μg/ml for 24, 48 and 72 h. Following treatment, CCK-8 was added and incubated with the cells at 37˚C for 2 h. The optical density was measured at 450 nm using Synergy H1 microplate reader (BioTek Instruments, Inc.) and calculated as follows: Inhibitory rate (%)=[1-(TB-treat OD-blank OD)/(untreated OD-blank OD)] x100%.

Clone formation assay. The U2OS cells were seeded into 6-well plates in triplicate (1,000 cells/well) for 48 h adherence and then treated with TB at 0, 5 and 10 μg/ml for 3 h. Following treatment, the cells were washed with PBS and the medium was replaced with fresh medium. In the following 8 days, the cells were treated TB for a further 3 times. The cell colonies were fixed with paraformaldehyde (4%) at 4˚C for 20 min and stained with 0.1% crystal violet at room temperature for 20 min (Sigma-Aldrich; Merck KGaA).

Cell cycle analysis. The U2OS cells were seeded in 10 cm dishes ($1.5x10^6$ cells/dish) for 24 h adherence and were synchronized by 10 μM Nocodazole for 8 h. The cells were then treated with TB at 12.5, 25 and 50 μg/ml for 12, 24 and 48 h. Subsequently, the cells were washed with PBS and fixed with 70% ice-cold ethanol overnight at -20˚C. Fixed cells were washed in PBS and stained with Propidium iodide/RNase Staining Buffer for 15 min at room temperature, followed by analysis using a BD Accuri™ C6 flow cytometer (BD Biosciences).

Immunofluorescence. The cell cytoskeleton of U2OS cells treated with TB was observed using Anti-Tubulin antibody-Microtubule Marker and Acti-stain™ Fluorescent Phalloidins. Briefly, the cells ($4x10^4$) were fixed with 4% paraformaldehyde for 15 min at room temperature and then permeabilized with PBS containing 0.1% Triton X-100 at 4˚C for 10 min. The cells were blocked with 1% BSA in tris-buffered saline-Tween 20 (TBST) solution at 4˚C for 1 h, and were then incubated with the anti-tubulin antibody (1:100, v/v) and anti-NF-κB antibody (1:400, v/v) at 4˚C overnight. Subsequently, Fluorescein (FITC)-conjugated AffiniPure Donkey Anti-Rabbit IgG (H+L) (1:2,000, v/v) was added to the cells incubated with anti-NF-κB antibody at 4˚C in dark for 2 h. The cells were incubated with Acti-stain™ 535 Phalloidin (100 nM) at room temperature for 30 min. Finally, the cells on coverslip slides were stained with ProLong Diamond Antifade Mountant with DAPI at room temperature overnight and observed under a fluorescence microscope (Zeiss AG). TNF-α (10 ng/ml) was used to stimulate the microfilament and microtubule formation of U2OS cells for 12 h as a model, and confocal laser scanning microscopy was employed to observe the effects of TB. The cells incubated with Phalloidin were observed under a Leica TCS SP5 confocal laser scanning microscope (Leica Microsystems GmbH) at settled excited wavelength (DAPI 405 nm, FITC 488 nm) and consistent detecting wave band (DAPI 420-470 nm, FITC 503-550 nm).

Cell migration and invasion assay. Cell migration assay and invasion assay were performed using a Transwell chamber system without and with Matrigel, respectively (Corning Costar, Inc.). The cells were starved in serum-free medium for 12 h and seeded into the upper chambers at $5x10^4$ cells/well

Table II. Gene expression in zebrafish differed significantly between the model group and TB-treated group (model vs. TB) in RNA sequencing analysis.

Gene name	log2 (fold change)	P-value	Adjusted P-value	Direction to model
MYH2	-1.868	3.24E-116	1.86E-114	Down
MYH7	-1.046	1.08E-109	5.57E-108	Down
TUBA1B	-1.234	7.82E-17	8.78E-16	Down
TUBB2A	-4.728	3.41E-29	6.30E-28	Down

in serum-free medium. Complete medium containing TB was added to the lower chambers and incubated with the upper chambers at 37˚C for 12 h without Matrigel and for 24 h with Matrigel. The migrated cells were then fixed with 4% paraformaldehyde and stained with 0.1% crystal violet at room temperature for 20 min for counting under an optical microscope (Zeiss AG).

Wound healing assay. The cells were seeded into 6-well plates ($5x10^5$ cells/well) and cultured for 24 h, followed by ab artificial scratch being made in a cross form using a micropipette tip. The cells were then cultured with fresh medium containing 0.5% FBS and TB at 10, 20 and 40 μg/ml. The cells were observed and imaged at 5 different time points (0, 12, 24 and 48 h) under an inverted microscope (Zeiss AG). The wound area was calculated using Image J 1.47 software. Each experiment was conducted in triplicate.

Western blot analysis. Total proteins were extracted from the TB-treated U2OS cells ($1.5x10^6$) using RIPA lysis buffer with proteinase inhibitor cocktail and phosphatase inhibitor cocktail for 30 min on ice. The proteins were quantified using the Pierce BCA Protein Assay kit, separated by electrophoresis and transferred onto polyvinylidene fluoride membranes (30 μg protein per lane). The membranes were blocked with 5% non-fat milk or 5% BSA for 2 h at 4˚C, followed by overnight incubation at 4˚C with primary antibodies (Vimentin, Slug, Snail, Claudin-1, ZEB1, E-Cadherin, N-Cadherin, IKKα, IKKβ, IκBα, NF-κB, phospho-IKKα/β, phospho-IκBα and Histone-H3) at dilution rate of 1:20,000 (v/v). The membranes were then washed 3 times with TBST for 5 min and incubated with Peroxidase AffiniPure Goat Anti-Mouse IgG (H+L) (1:20,000, v/v) at 4˚C for 2 h. Target proteins were visualized using Immobilon Western Chemiluminescent HRP Substrate and detected using X-ray film and scanned. The densitometry of each blot was tested by using ImageJ software (version 1.8.0).

Statistical analysis. Data are expressed as the means ± SD and analyzed by a normal distribution test, followed by one-way ANOVA coupled with Dunnett's multiple comparisons test. All analyses were performed using GraphPad Prism 8.0. A value of $P<0.05$ was considered to indicate a statistically significant difference.

Results

RNA-seq-based transcriptional action of TB. The tumor-inhibitory effect of TB on U2OS cells in zebrafish has been previously reported (17). In the present study, by using RNA samples from model group and TB (2.13 μg/ml)-treated group, RNA-seq analysis was performed by Gene Ontology analysis. The results revealed that TB regulated a number of biological processes, in which the microtubule bundle formation was inhibited (Fig. S1). As shown in Table II, a number of genes involved in the microtubule bundle formation of U2OS cells, including *MYH2*, *MYH7*, *TUBA1B* and *TUBB2A*, were significantly downregulated by treatment with TB, indicating the inhibition of microtubule bundle formation by TB. To verify this result, RT-qPCR was performed and a similar result was obtained, in that the expression levels of all these genes were significantly downregulated following treatment with TB (each $P<0.01$) (Fig. 1).

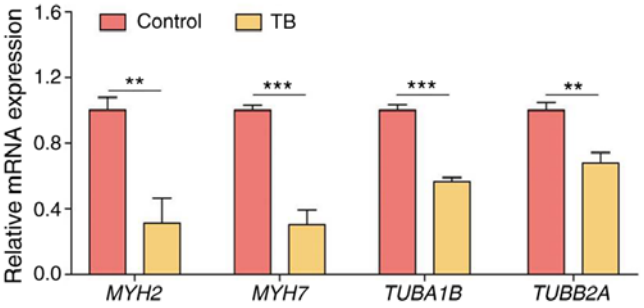

Figure 1. Relative mRNA expression levels of genes for the microtubule bundle formation of U2OS cells. Data are shown as the means ± SD. $^{**}P<0.01$ and $^{***}P<0.001$ vs. control. TB, theabrownin.

Anti-colony formation and cell cycle-arresting effects of TB. As shown in Fig. 2A, the viability of the U2OS cells was significantly inhibited by TB and the inhibitory rate was increased with the increasing concentrations of TB from 10 to 100 μg/ml, and with the increasing treatment duration from 24 to 72 h. It was found that TB exerted anti-proliferative effects in a dose-dependent and time-dependent manner. As shown in Fig. 2B, the results of colony formation assay revealed that TB at 5 μg/ml significantly decreased the U2OS cell colony numbers (>50 cells/colony; $P<0.001$), and there was almost no colony formation observed following treatment with TB at 10 μg/ml. As shown in Fig. 2C and D, TB blocked the cell cycle progression of U2OS cells at the G_2/M phase from 12 to 48 h. With the increasing concentration of TB, the G_2/M phase cell percentage progressively increased when compared with the control.

Cytoskeleton-inhibitory effects of TB. According to the result of RNA-seq analysis, the inhibition of microtubule

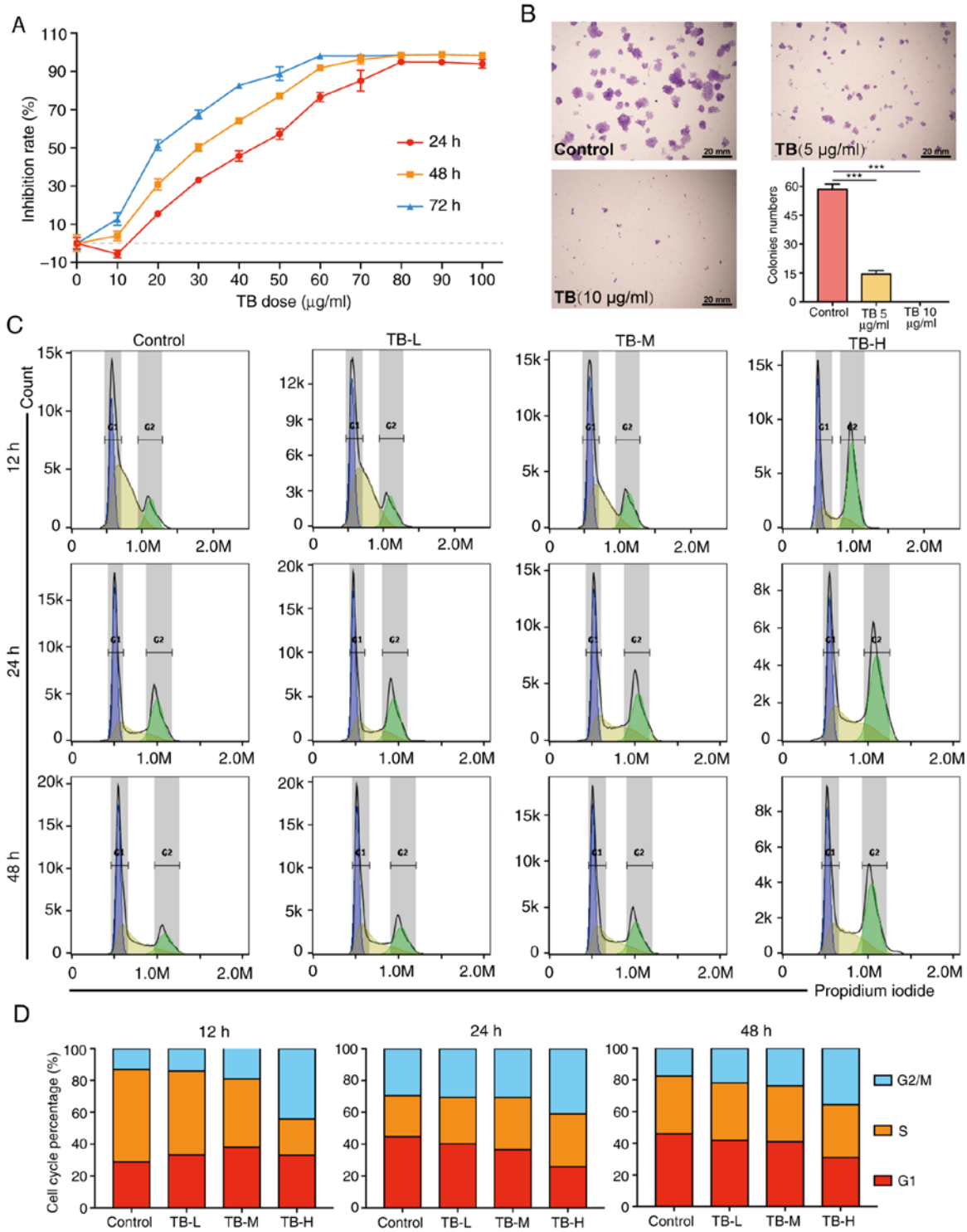

Figure 2. (A) Cell viability, (B) colony formation assay, (C) cell cycle analysis and (D) cell cycle percentage of U2OS cells treated with TB. Data are shown as the means ± SD. ***P<0.001 vs. control. TB, theabrownin.

bundle formation was the primary effects through which TB affected U2OS cells and zebrafish. To confirm this effect, immunofluorescence using antibodies against cytoskeleton proteins was performed. As shown in Fig. 3A and B, the cellular expression of Tubulin and F-actin was markedly decreased, with the visible loss of microfilament and microtubule bundles induced by TB at 12.5 to 50 μg/ml, indicating that TB exerted cytoskeleton-inhibitory effects on the U2OS cells. This effect was significantly exerted by TB at 25 (TB-L) and 50 μg/ml (TB-H) (each P<0.001) (Fig. 3C and D).

To further confirm the cytoskeleton-inhibitory effects of TB, A TNF-α-induced microfilament- and microtubule-formation model was applied. As shown in Fig. 4, the fluorescence intensity of F-actin and the formation of microfilaments were evidently increased with TNF-α pre-treatment, and the phenotype was reversed to normal by treatment with TB, verifying the inhibitory effects of TB on the cytoskeleton.

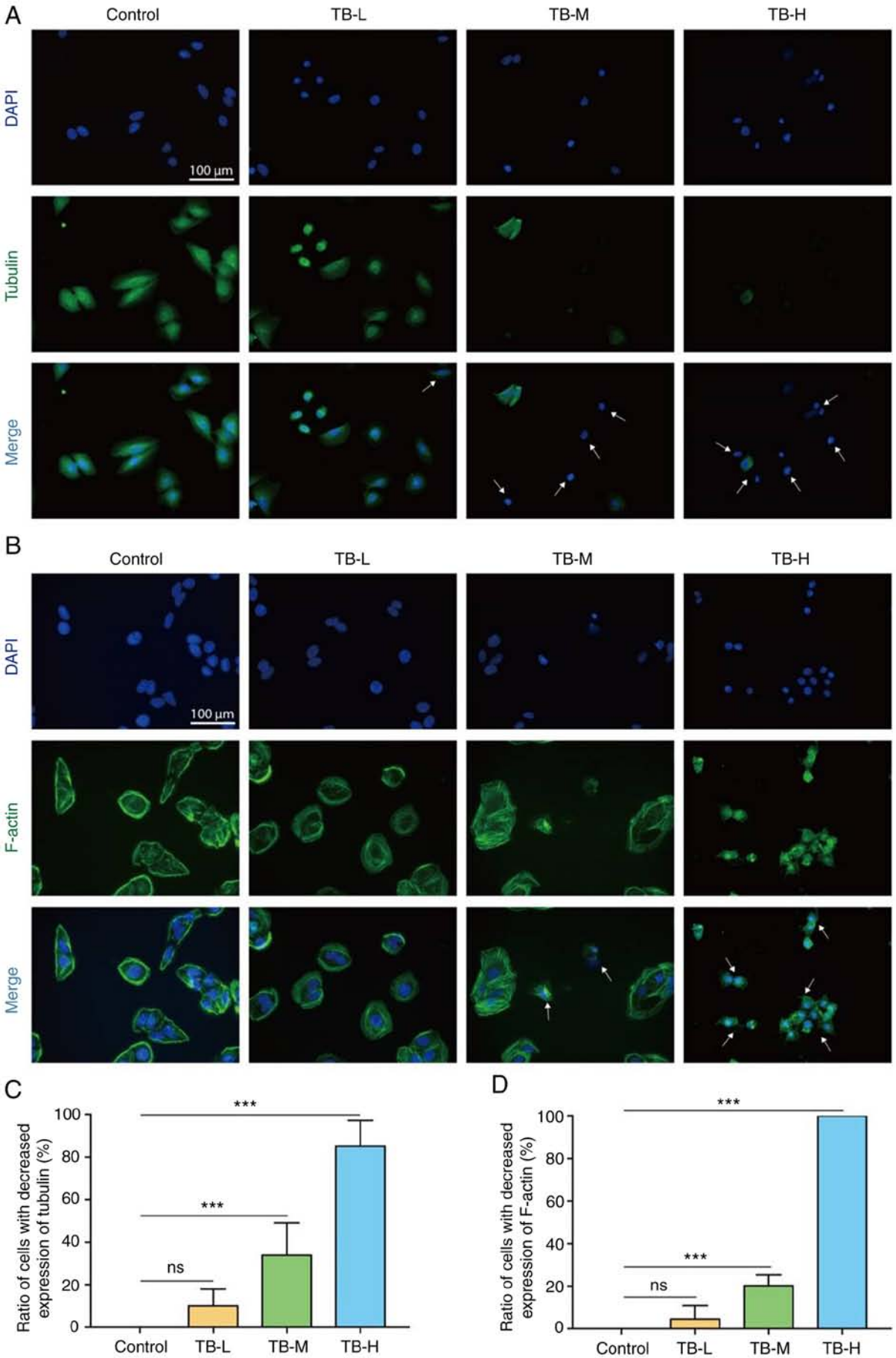

Figure 3. Immunofluorescence expression of Tubulin (A) and F-actin (B) on U2OS cells and the ratio of abnormal cells with downregulated Tubulin (C) and the ratio of abnormal cells with downregulated F-actin (D) Data are shown as the means ± SD. Arrows indicate abnormal cells. ***P<0.001 vs. control. TB, theabrownin; ns, not significant; TB-L, 25 μg/ml; TB-H, 50 μg/ml.

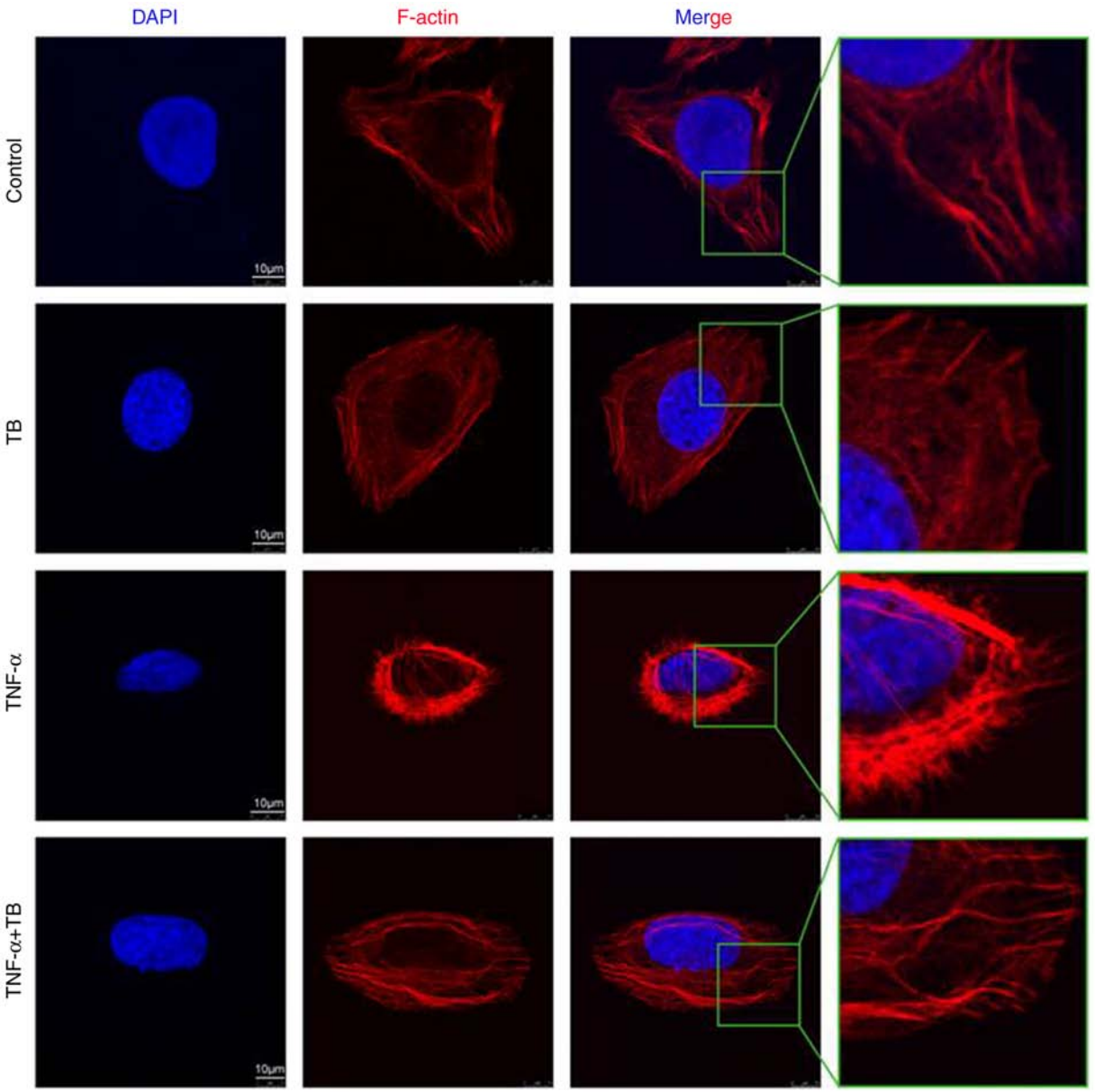

Figure 4. Detection of F-actin expression and microfilament bundles by confocal laser scanning microscopic observation. TB, theabrownin.

Anti-migratory and anti-invasive effects of TB. The integrities of microfilament and microtubule formation are crucial for the functions of cell migration and invasion, which may be disrupted by TB in U2OS cells. To determine whether TB exerts inhibitory effects on the migration and invasion of the U2OS cells, Transwell and wound healing assays were performed. As shown in Fig. 5, TB significantly inhibited the migration of U2OS cells following 12 h of treatment at the middle and high doses, and significantly inhibited U2OS cell invasion following treatment for 24 h treatment at the low, middle and high doses, with significant decreases observed in the numbers of migrated and invaded cells (each $P<0.001$). Moreover, the results of CCK-8 assays revealed that TB at these concentrations had no significant effect on the viability of the U2OS cells, indicating that the anti-migratory and anti-invasive effects of TB were independent on its anti-proliferative effects. As shown in Fig. 6, TB significantly inhibited the wound healing ability of the U2OS cells following 12 h of treatment at the middle and high doses, and following 24 and 48 h of treatment at the low, middle and high doses (each $P<0.05$). These results indicated that TB inhibited U2OS cell migration through the blockage of wound closure in a dose-dependent manner.

Molecular mechanisms of TB. To clarify the underlying mechanisms of the anti-migratory and anti-invasive effects of TB, western blot analysis was conducted on the proteins involved in epithelial-mesenchymal transition (EMT) and the related pathways. As shown in Fig. 7A and B, the expression levels of vimentin, Slug, Snail-1, ZEB-1 and β-catenin were significantly downregulated, while those of Claudin-1 and E-cadherin were significantly upregulated by TB at 25 and 50 μg/ml, indicating that the anti-migratory and anti-invasive effects of TB were mediated by the reversal of EMT. Moreover, the levels of key molecules in the NF-κB pathway, including cytoplasmic NF-κB, nuclear NF-κB, IKKα, phospho-IKKα (p-IKKα), phospho-IKKβ (p-IKKβ), and phospho-IκBα (p-IκBα),

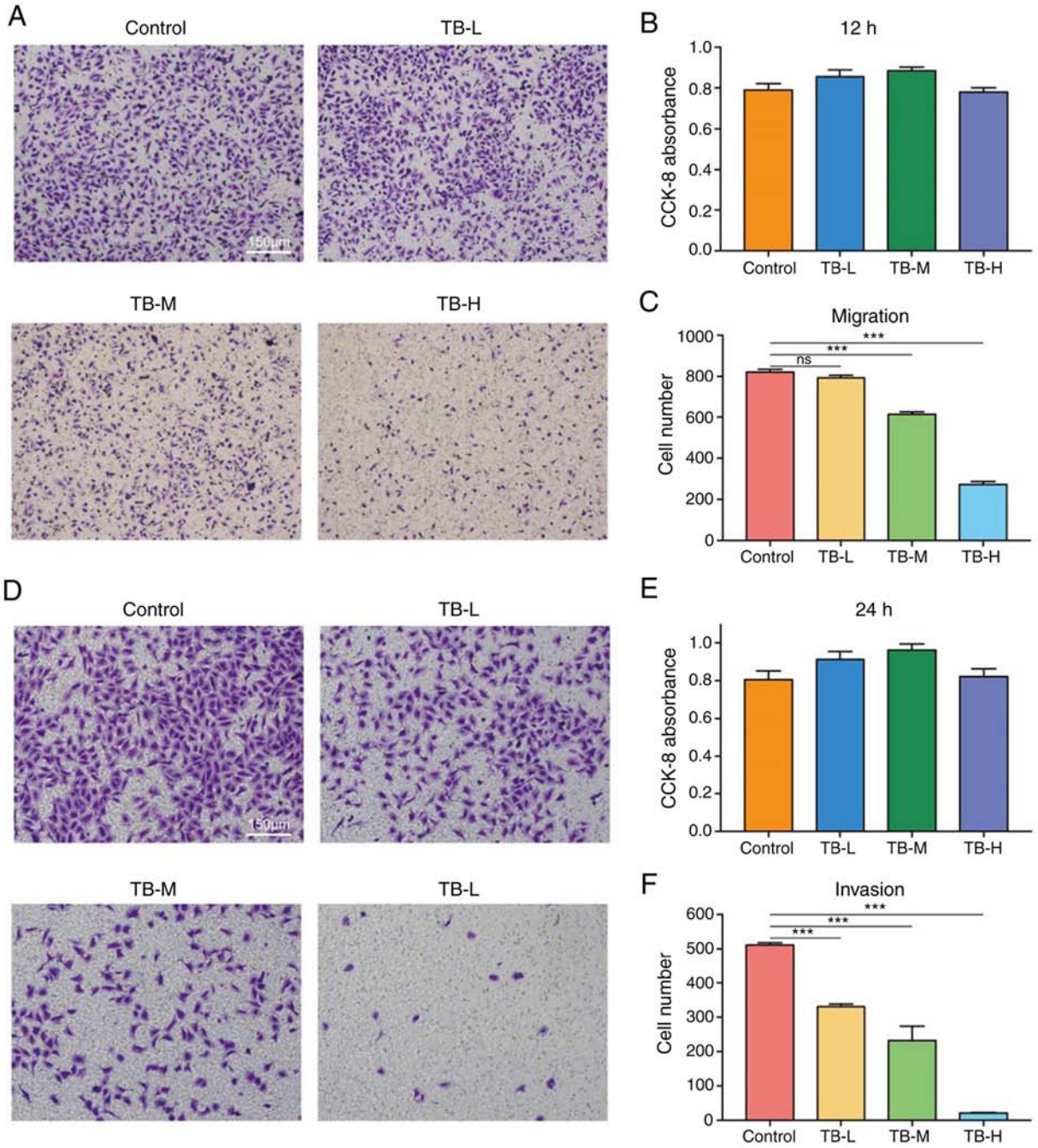

Figure 5. (A) Migration assay, CCK-8 assay (B) and migrated cell number (C) of U2OS cells at 12 h; invasion assay (D) CCK-8 assay (E) and invaded cell number (F) of U2OS cells at 24 h. Data are shown as the means ± SD. ***P<0.001 vs. control. TB, theabrownin; ns, not significant; TB-L, 2.5 μg/ml; TB-M, 5 μg/ml; TB-H, 10 μg/ml.

were all significantly downregulated by TB (Fig. 7C and D), indicating that NF-κB pathway may participate in the mechanisms of TB. As shown in Fig. S2, the immunofluorescent data verified that TB inhibited NF-κB in U2OS cells. The above-mentioned results revealed that the mechanisms of TB were mediated by the reversal of EMT and associated with the inhibition of NF-κB signaling (Fig. 8).

Discussion

In a previous study, the authors demonstrated that the pro-apoptotic and tumor-inhibitory effects and p53 signaling pathway-dependent mechanism of TB on osteosarcoma, providing a promising candidate pro-apoptotic anti-osteosarcoma agent (17). Considering the high metastatic potential of osteosarcoma, both pro-apoptotic and anti-metastatic effects are important and needed for anti-osteosarcoma therapy. However, to the best of our knowledge, there are no available drugs that effectively inhibit the metastases of osteosarcoma. For the first time, to the best of our knowledge, the present study evaluated the anti-metastatic potential of TB by exploring its inhibitory effects on the metastasis-associated activities of osteosarcoma cells and the related mechanisms. Biologically, it was found that TB significantly inhibited the colony formation,

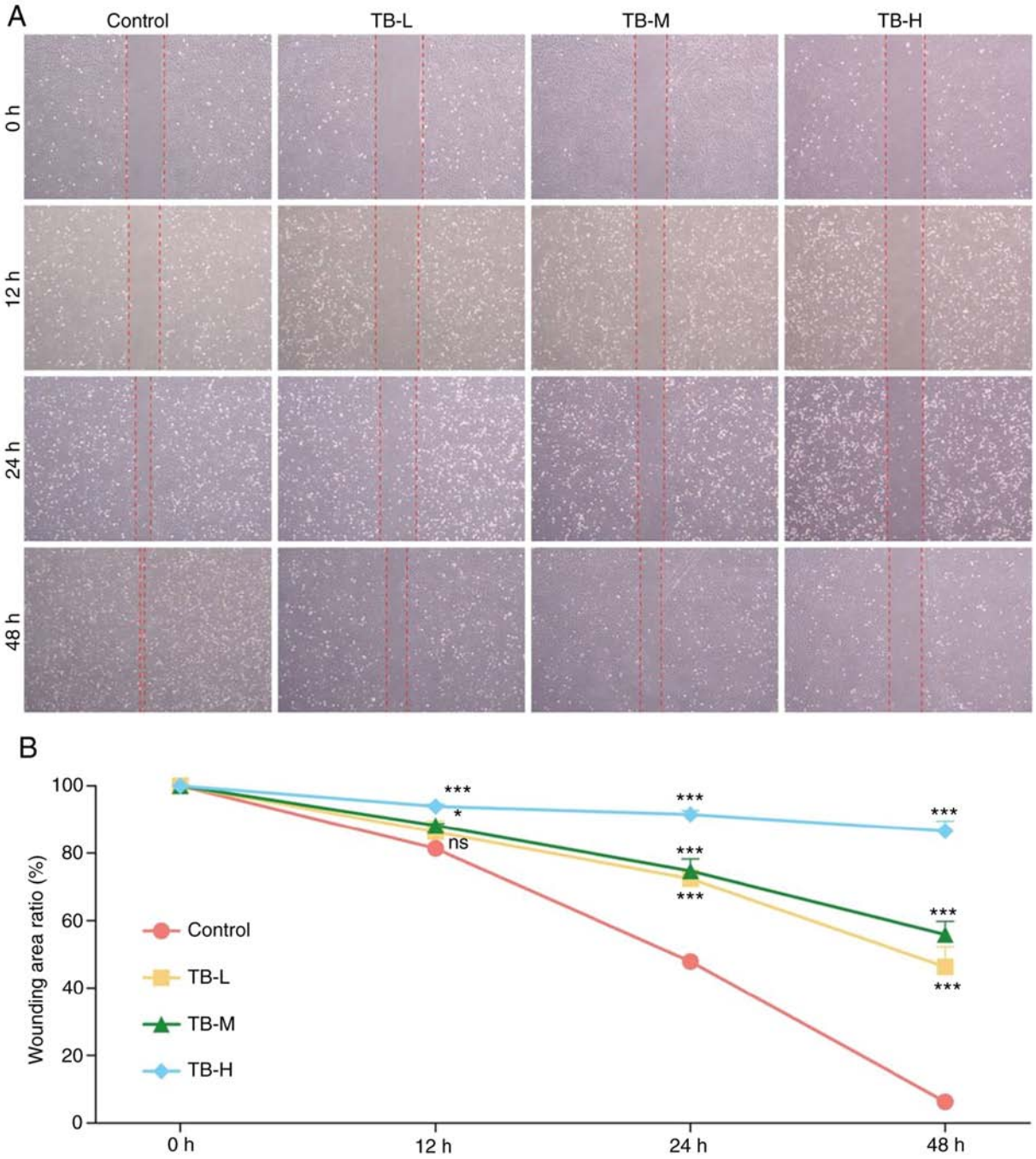

Figure 6. Wound healing assay (A) and wounding area ratio (B) of U2OS cells treated with TB. Data are shown as the means ± SD. *P<0.05 and ***P<0.001 vs. control. TB, theabrownin; ns, not significant; TB-L, 10 μg/ml; TB-M, 20 μg/ml; TB-H, 40 μg/ml.

cell cycle transition, microtubule and microfilament formation, migration and invasion of U2OS osteosarcoma cells, indicating its anti-migratory and anti-invasive effects. On a molecular level, it was revealed that the anti-migratory and anti-invasive mechanisms of TB was mediated by the reversal of EMT and associated with the inhibition of NF-κB signaling (Fig. 8). The innovative contribution of the present study is the discovery of the cytoskeleton-specific anti-migratory and anti-invasive effects and mechanisms of TB, which provide a promising candidate for both pro-apoptotic and anti-metastatic purposes for the treatment of osteosarcoma.

EMT was originally described in the early 1980s as a biological process through which epithelial cells lose their epithelial characteristics and acquire mesenchymal characteristics (20). During EMT, epithelial cells lose their junctions and apical-basal polarity, reorganize their cytoskeleton, undergo a change in cell shape and alter their gene expression, and increase the motility and invasiveness of individual cells (21,22). EMT is activated during wound healing, fibrosis and cancer progression (23,24). A number of studies have indicated that EMT plays a vital role in the metastatic initiation of several types of cancer, such as osteosarcoma, by enabling tumour cells to gain invasive properties and metastatic growth characteristics (25). The major events in EMT are the loss of E-cadherin, the translocation of β-catenin from the cell membrane to the nucleus, and the activation of vimentin,

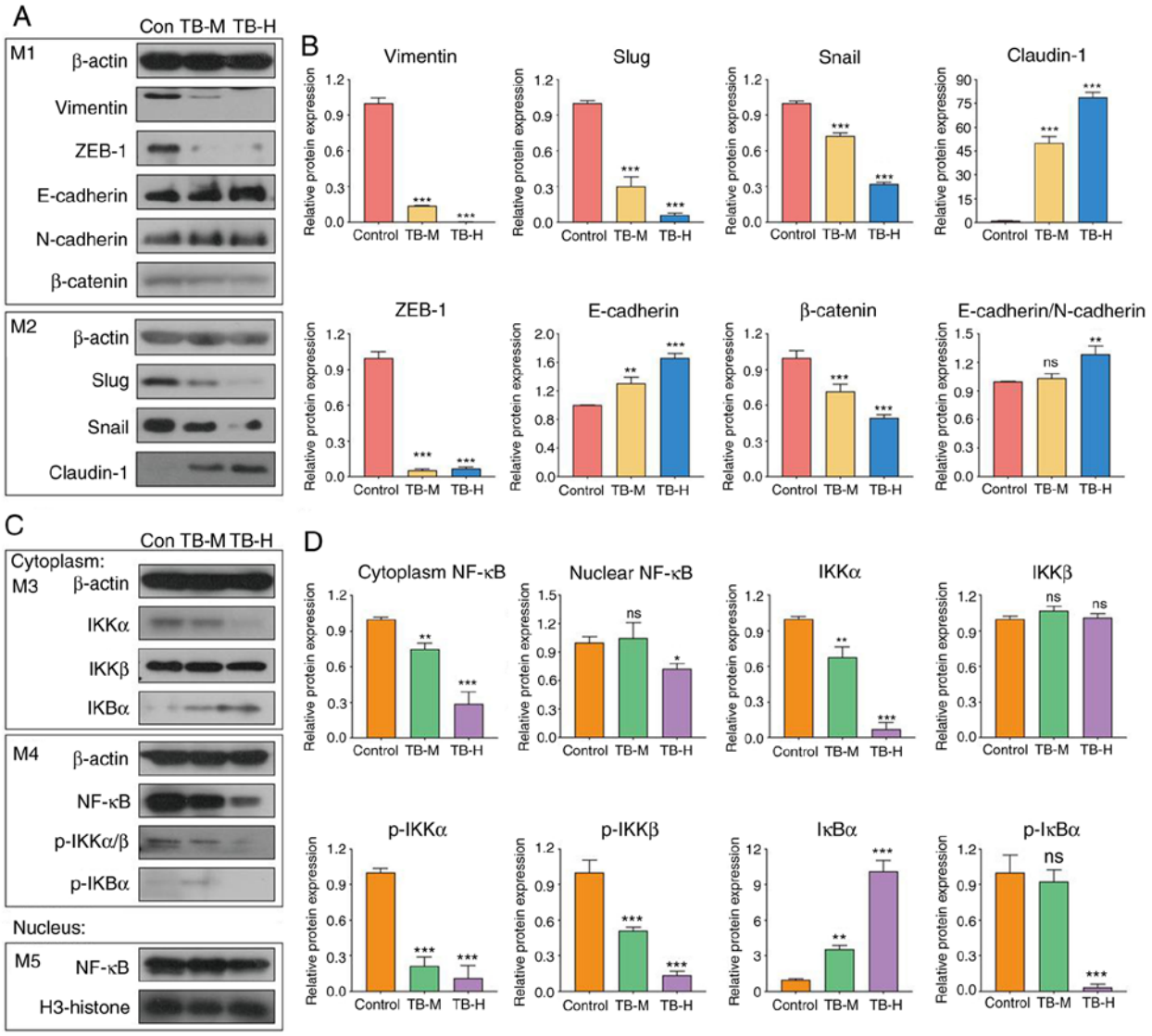

Figure 7. Expression and phosphorylation of TB-targeted proteins in U2OS cells following 24 h treatment. (A) Expression profile of EMT-related proteins; (B) Statistical analysis of EMT-related protein expression; (C) Expression profile of NF-κB pathway-related proteins; (D) Statistical analysis of NF-κB pathway-related protein expression. Data are shown as the means ± SD. *P<0.05, **P<0.01 and ***P<0.001 vs. control. The bands obtained from one membrane was placed in the same box (M1, M2, M3 and M4). TB, theabrownin; ns, not significant; TB-M, 25 μg/ml; TB-H, 50 μg/ml.

induced by transcription factors, such as Snail-1, Slug and ZEB-1 (26,27). E-cadherin is a 120 kDa Ca^{2+}-dependent transmembrane glycoprotein present on the surface of epithelial cells and mediates cell-cell adhesion at adherens junctions through homophilic binding, thus maintaining epithelial cellular adhesion and integrity to support the tissue architecture (28). The cytoplasmic domain of E-cadherin interacts with α, β and γ catenins to act on the actin cytoskeleton in cells (29). E-cadherin switching is indispensable during EMT, and the loss or suppression of E-cadherin expression leads to cancer development and progression, as well as metastasis (30-32). Moreover, as a major cytoskeletal protein in the large intermediate filament, vimentin is important for the structural integrity of tumour cells and is often overexpressed at the end stages of progression in EMT, representing the highly proliferative and invasive characteristics of tumour cells (33). Conversely, the knockdown of vimentin with antisense oligonucleotides reduces cell motility (34). In the present study, the expression of E-cadherin and E-cadherin/N-cadherin was upregulated, and that of vimentin and β-catenin was downregulated by TB, indicating that the mechanisms of TB are mediated by the suppression of EMT. Snail proteins, including Snail-1 and Slug (also known as Snail-2), are zinc finger-containing transcription factors that act as repressors of E-cadherin by binding to the E-box (5'-CACCTG-3') in the E-cadherin promoter (35). Snail and Slug are overexpressed in osteosarcoma and induce EMT by downregulating E-cadherin, leading to an increase in cell migration, invasion and tumour progression of osteosarcoma (35-37). The ZEB family (ZEB-1 and ZEB-2) is another group of zinc finger transcription factors targeting the E-box and E-box-like DNA sequences in the target gene promoters (38). ZEB proteins induce EMT by downregulating E-cadherin, which is overexpressed, and plays critical roles in cell proliferation, migration and progression of osteosarcoma (39,40). In the present study, TB downregulated the expression of Snail-1, Slug and ZEB-1, indicating that

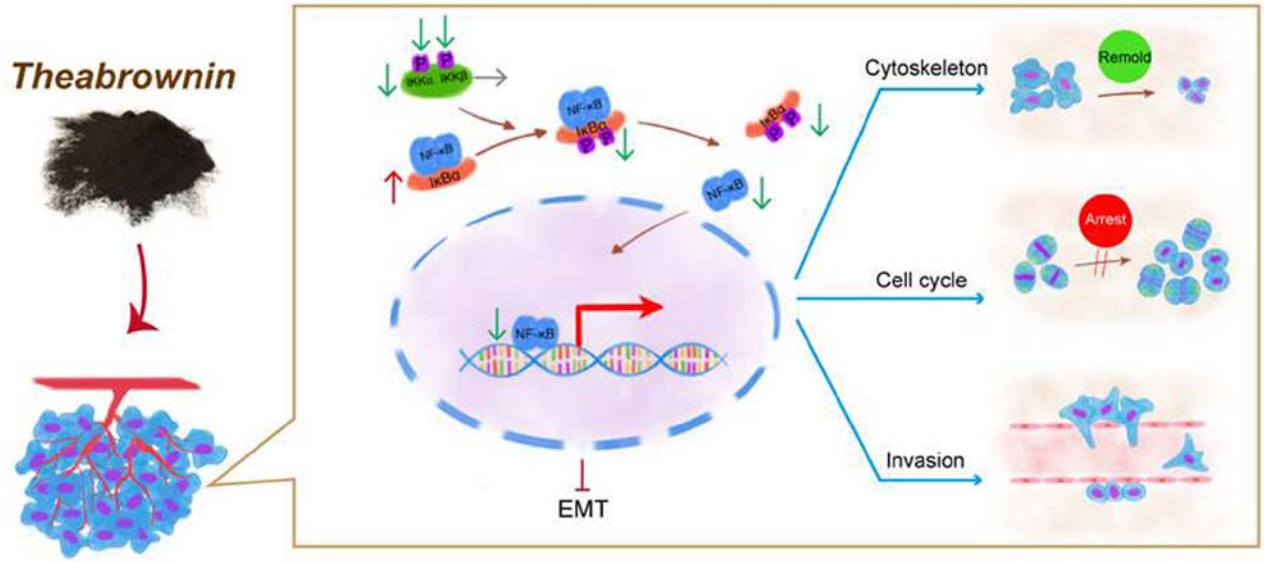

Figure 8. Overview of the effects and mechanisms of TB on osteosarcoma cells. TB, theabrownin; EMT, epithelial-mesenchymal transition.

Snails/ZEB-E-cadherin/β-catenin are the targets of TB in osteosarcoma treatment.

Emerging evidence has indicated that the NF-κB signaling pathway plays central roles in the control of cell growth, apoptosis, stress response, and several other physiological processes (41,42). It protects tumour cells from apoptosis, while also supporting cell invasion, metastasis, and angiogenesis of tumour cells (43,44). In addition, the activation of the NF-κB pathway has been confirmed as an essential step towards EMT in tumor cells. NF-κB directly leads to EMT in tumor cells by activating the transcription of *SNAIL* and *ZEB-1*, resulting in *E-cadherin* suppression and vimentin overexpression (33,45,46). The underlying mechanisms of the association between NF-κB and EMT have been clarified, in which the phosphorylation of IκB increases the abundance of nuclear-localized NF-κB to promote the expression of *SNAIL* and *ZEB-1* (47). Therefore, the NF-κB signaling pathway is essential for tumor invasion and metastasis via EMT (48). Conversely, the inhibition of the NF-κB pathway can induce a 10-fold reduction in the metastasis of cancer due to the blockage of EMT (33,49). In the present study, TB inhibited the NF-κB pathway by downregulating NF-κB, IKKα, p-IKKα, p-IKKβ and p-IκBα in U2OS cells, resulting in EMT blockade with the downregulation of vimentin, Slug, Snail-1, ZEB-1 and β-catenin (Fig. 7). The cytoplasm and nuclear NF-κB data indicated that TB not only blocked the transition of NF-κB from the cytoplasm to the nucleus, but also inhibited the total expression of NF-κB. The cell immunofluorescent data provided evidence of this conclusion (Fig. S2). The results indicated that the NF-κB pathway may participate in the EMT-mediated anti-osteosarcoma mechanisms of TB (Fig. 8). A key question remains however, as to what connects TB and NF-κB. Most likely, receptors on the osteosarcoma cell membrane, such as CXCR4, endothelin-1 receptors (ET_A), adenosine A3 receptor (A3AR), Toll-like receptor 4 (TLR4) and estrogen receptor β (ERβ), are the answer. CXCR4 is an SDF-1 receptor overexpressed in human osteosarcoma cells that mediates the migration of osteosarcoma cells by inducing IκB kinase (IKKα/β) phosphorylation, IκB phosphorylation, p65 phosphorylation and κB-luciferase activity in the NF-κB pathway (50). As an ET-1-specific receptor, ET_A controls the invasive ability of osteosarcoma cells through matrix metalloproteinases (MMPs; MMP-2 and MMP-9) and NF-κB transcription factors, and targeting this receptor may prove to be a significant treatment strategy for osteosarcoma (51). A3AR expression is lower in human osteosarcoma tissues than in normal tissues, and it acts as a suppressor of osteosarcoma migration and progression by inhibiting the PKA/Akt/NF-κB axis (52). TLR4 is an upstream receptor of the MAPK/NF-κB pathway in human osteosarcoma cells, and the inhibition of TLR4 expression exerts suppressive effets on osteosarcoma (53). ERβ has been found to exert evident anti-tumor effects on osteosarcoma cells by regulating the integrin, PI3K/Akt and NF-κB signal pathways, and the viability, migration and invasion of U2OS cells can be significantly inhibited by ERβ agonists (54). These receptors may be potential targets of TB for the modulation of the NF-κB pathway in U2OS cells, warranting further investigation.

In conclusion, to the best of our knowledge, the present study is the first to demonstrate the inhibitory effects of TB on the cytoskeleton-dependent cell cycle, migration and invasion of human osteosarcoma cells. The mechanisms of TB were found to be mediated by the suppression of EMT, which may be associated with the NF-κB pathway. Therefore, TB can be regarded as an anti-metastatic agent for the treatment of osteosarcoma. Considering that only one osteosarcoma cell line was used in the present study, further studies are required to determine the anti-metastatic effects of TB on other tumor cell lines. In particular, *in vivo* studies are also required in the future to verify these effects of TB. Taken together, the findings of the present study provide novel evidence of the anti-osteosarcoma effects of TB and contribute to the development of natural product-derived anti-metastatic agents for osteosarcoma therapy.

Acknowledgements

Not applicable.

Funding

The present study was supported by the National Natural Science Foundation of China (grant nos. 81774331 and 81873049), the Zhejiang Provincial Natural Science Foundation of China (grant nos. LY18H270016, LY18H270004 and LY17H270001), the Medical Health Science and Technology Project of Zhejiang Provincial Health Commission (grant no. 2012ZA045); and the Zhejiang Provincial Key Construction University Superiority Characteristic Discipline (Traditional Chinese Pharmacology) Opening Foundation of China (grant no. ZYX2018006).

Availability of data and materials

All data generated or analyzed during this study are included in this published article or are available from the corresponding author on reasonable request.

Authors' contributions

WJ conducted the main work of the cellular and molecular experiments and contributed to the revision of this manuscript. CG, LZ, XY and MG contributed to the cellular and molecular experiments. JZ provided the TB and improved the experimental design of the study. JC and XD were involved in the conception of the study. QY was involved in the conception of the study and provided funding to support to the study. LS designed the study, drafted and revised the manuscript, and provided funding support to the study. All listed authors approved the manuscript for publication, and agree to be accountable for all aspects of the study.

Ethics approval and consent to participate

The zebrafish larvae used in the present study were <5 days post-fertilization and thus were not free-feeding and thus do not count as a protected species. Thus, ethics approval was not required for the zebrafish experiments in the present study, as the larvae were sacrificed at 4 days post-fertilization.

Patient consent for publication

Not applicable.

Competing interests

The authors declare that they have no competing interests.

References

1. Mirabello L, Troisi RJ and Savage SA: Osteosarcoma incidence and survival rates from 1973 to 2004: Data from the surveillance, epidemiology, and end results program. Cancer 115: 1531-1543, 2009.
2. Mirabello L, Troisi RJ and Savage SA: International osteosarcoma incidence patterns in children and adolescents, middle ages and elderly persons. Int J Cancer 125: 229-234, 2009.
3. Valery PC, Laversanne M and Bray F: Bone cancer incidence by morphological subtype: A global assessment. Cancer Causes Control 26: 1127-1139, 2015.
4. Bielack SS, Kempf-Bielack B, Delling G, Exner GU, Flege S, Helmke K, Kotz R, Salzer-Kuntschik M, Werner M, Winkelmann W, *et al*: Prognostic factors in high-grade osteosarcoma of the extremities or trunk: An analysis of 1,702 patients treated on neoadjuvant cooperative osteosarcoma study group protocols. J Clin Oncol 20: 776-790, 2002.
5. Whelan JS, Bielack SS, Marina N, Smeland S, Jovic G, Hook JM, Krailo M, Anninga J, Butterfass-Bahloul T, Böhling T, *et al*: EURAMOS-1, an international randomised study for osteosarcoma: Results from pre-randomisation treatment. Ann Oncol 26: 407-414, 2015.
6. Guo J, Reddick WE, Glass JO, Ji Q, Billups CA, Wu J, Hoffer FA, Kaste SC, Jenkins JJ, Ortega Flores XC, *et al*: Dynamic contrast-enhanced magnetic resonance imaging as a prognostic factor in predicting event-free and overall survival in pediatric patients with osteosarcoma. Cancer 118: 3776-3785, 2012.
7. Le Vu B, de Vathaire F, Shamsaldin A, Hawkins MM, Grimaud E, Hardiman C, Diallo I, Vassal G, Bessa E, Campbell S, *et al*: Radiation dose, chemotherapy and risk of osteosarcoma after solid tumours during childhood. Int J Cancer 77: 370-377, 1998.
8. Calvert GT, Randall RL, Jones KB, Cannon-Albright L, Lessnick S and Schiffman JD: At-risk populations for osteosarcoma: The syndromes and beyond. Sarcoma 2012: 152382, 2012.
9. Klein MJ and Siegal GP: Osteosarcoma: Anatomic and histologic variants. Am J Clin Pathol 125: 555-581, 2006.
10. Meyers PA, Schwartz CL, Krailo M, Kleinerman ES, Betcher D, Bernstein ML, Conrad E, Ferguson W, Gebhardt M, Goorin AM, *et al*: Osteosarcoma: A randomized, prospective trial of the addition of ifosfamide and/or muramyl tripeptide to cisplatin, doxorubicin, and high-dose methotrexate. J Clin Oncol 23: 2004-2011, 2005.
11. Kempf-Bielack B, Bielack SS, Jurgens H, Branscheid D, Berdel WE, Exner GU, Göbel U, Helmke K, Jundt G, Kabisch H, *et al*: Osteosarcoma relapse after combined modality therapy: An analysis of unselected patients in the cooperative osteosarcoma study group (COSS). J Clin Oncol 23: 559-568, 2005.
12. Jensen GS, Beaman JL, He Y, Guo Z and Sun H: Reduction of body fat and improved lipid profile associated with daily consumption of a Puer tea extract in a hyperlipidemic population: A randomized placebo-controlled trial. Clin Interv Aging 11: 367-376, 2016.
13. Yang M, Wang C and Chen H: Green, oolong and black tea extracts modulate lipid metabolism in hyperlipidemia rats fed high-sucrose diet. J Nutr Biochem 12: 14-20, 2001.
14. Wu LY, Juan CC, Hwang LS, Hsu YP, Ho PH and Ho LT: Green tea supplementation ameliorates insulin resistance and increases glucose transporter IV content in a fructose-fed rat model. Eur J Nutr 43: 116-124, 2004.
15. Imai K, Suga K and Nakachi K: Cancer-preventive effects of drinking green tea among a Japanese population. Prev Med 26: 769-775, 1997.
16. Nakachi K, Suemasu K, Suga K, Takeo T, Imai K and Higashi Y: Influence of drinking green tea on breast cancer malignancy among Japanese patients. Jpn J Cancer Res 89: 254-261, 1998.
17. Jin W, Zhou L, Yan B, Yan L, Liu F, Tong P, Yu W, Dong X, Xie L, Zhang J, *et al*: Theabrownin triggers DNA damage to suppress human osteosarcoma U2OS cells by activating p53 signalling pathway. J Cell Mol Med 22: 4423-4436, 2018.
18. Zhou L, Wu F, Jin W, Yan B, Chen X, He Y, Yang W, Du W, Zhang Q, Guo Y, *et al*: Theabrownin inhibits cell cycle progression and tumor growth of lung carcinoma through c-myc-Related mechanism. Front Pharmacol 8: 75, 2017.
19. Livak KJ and Schmittgen TD: Analysis of relative gene expression data using real-time quantitative PCR and the 2(-Delta Delta C(T)) method. Methods 25: 402-408, 2001.
20. Hay ED: An overview of epithelio-mesenchymal transformation. Acta Anat (Basel) 154: 8-20, 1995.
21. Thiery JP and Sleeman JP: Complex networks orchestrate epithelial-mesenchymal transitions. Nat Rev Mol Cell Biol 7: 131-142, 2006.
22. Thiery JP, Acloque H, Huang RY and Nieto MA: Epithelial-mesenchymal transitions in development and disease. Cell 139: 871-890, 2009.
23. Lamouille S, Xu J and Derynck R: Molecular mechanisms of epithelial-mesenchymal transition. Nat Rev Mol Cell Biol 15: 178-196, 2014.

24. Chapman HA: Epithelial-mesenchymal interactions in pulmonary fibrosis. Annu Rev Physiol 73: 413-435, 2011.
25. Yang G, Yuan J and Li K: EMT transcription factors: Implication in osteosarcoma. Med Oncol 30: 697, 2013.
26. Peinado H, Olmeda D and Cano A: Snail, Zeb and bHLH factors in tumour progression: An alliance against the epithelial phenotype? Nat Rev Cancer 7: 415-428, 2007.
27. De Craene B and Berx G: Regulatory networks defining EMT during cancer initiation and progression. Nat Rev Cancer 13: 97-110, 2013.
28. Damsky CH, Richa J, Solter D, Knudsen K and Buck CA: Identification and purification of a cell surface glycoprotein mediating intercellular adhesion in embryonic and adult tissue. Cell 34: 455-466, 1983.
29. Kobielak A and Fuchs E: Alpha-catenin: At the junction of intercellular adhesion and actin dynamics. Nat Rev Mol Cell Biol 5: 614-625, 2004.
30. Oka H, Shiozaki H, Kobayashi K, Inoue M, Tahara H, Kobayashi T, Takatsuka Y, Matsuyoshi N, Hirano S, Takeichi M, *et al*: Expression of E-cadherin cell adhesion molecules in human breast cancer tissues and its relationship to metastasis. Cancer Res 53: 1696-1701, 1993.
31. Gumbiner BM: Cell adhesion: The molecular basis of tissue architecture and morphogenesis. Cell 84: 345-357, 1996.
32. Hirohashi S: Inactivation of the E-cadherin-mediated cell adhesion system in human cancers. Am J Pathol 153: 333-339, 1998.
33. Min C, Eddy SF, Sherr DH and Sonenshein GE: NF-kappaB and epithelial to mesenchymal transition of cancer. J Cell Biochem 104: 733-744, 2008.
34. Hendrix MJ, Seftor EA, Chu YW, Trevor KT and Seftor RE: Role of intermediate filaments in migration, invasion and metastasis. Cancer Metastasis Rev 15: 507-525, 1996.
35. Cano A, Perez-Moreno MA, Rodrigo I, Locascio A, Blanco MJ, del Barrio MG, Portillo F and Nieto MA: The transcription factor snail controls epithelial-mesenchymal transitions by repressing E-cadherin expression. Nat Cell Biol 2: 76-83, 2000.
36. Yang H, Zhang Y, Zhou Z, Jiang X and Shen A: Snail-1 regulates VDR signaling and inhibits 1,25(OH)-D_3 action in osteosarcoma. Eur J Pharmacol 670: 341-346, 2011.
37. Sharili AS, Allen S, Smith K, Hargreaves J, Price J and McGonnell I: Expression of Snail2 in long bone osteosarcomas correlates with tumour malignancy. Tumour Biol 32: 515-526, 2011.
38. Gheldof A, Hulpiau P, van Roy F, De Craene B and Berx G: Evolutionary functional analysis and molecular regulation of the ZEB transcription factors. Cell Mol Life Sci 69: 2527-2541, 2012.
39. Huang Y, Yang Y, Gao R, Yang X, Yan X, Wang C, Jiang S and Yu L: RLIM interacts with Smurf2 and promotes TGF-β induced U2OS cell migration. Biochem Biophys Res Commun 414: 181-185, 2011.
40. Arima Y, Inoue Y, Shibata T, Hayashi H, Nagano O, Saya H and Taya Y: Rb depletion results in deregulation of E-cadherin and induction of cellular phenotypic changes that are characteristic of the epithelial-to-mesenchymal transition. Cancer Res 68: 5104-5112, 2008.
41. Barnes PJ and Karin M: Nuclear factor-kappaB: A pivotal transcription factor in chronic inflammatory diseases. N Engl J Med 336: 1066-1071, 1997.
42. Karin M and Greten FR: NF-kappaB: Linking inflammation and immunity to cancer development and progression. Nat Rev Immunol 5: 749-759, 2005.
43. Huang S, Pettaway CA, Uehara H, Bucana CD and Fidler IJ: Blockade of NF-kappaB activity in human prostate cancer cells is associated with suppression of angiogenesis, invasion, and metastasis. Oncogene 20: 4188-4197, 2001.
44. Helbig G, Christopherson KW II, Bhat-Nakshatri P, Kumar S, Kishimoto H, Miller KD, Broxmeyer HE and Nakshatri H: NF-kappaB promotes breast cancer cell migration and metastasis by inducing the expression of the chemokine receptor CXCR4. J Biol Chem 278: 21631-21638, 2003.
45. Radisky DC and Bissell MJ: NF-kappaB links oestrogen receptor signalling and EMT. Nat Cell Biol 9: 361-363, 2007.
46. Chua HL, Bhat-Nakshatri P, Clare SE, Morimiya A, Badve S and Nakshatri H: NF-kappaB represses E-cadherin expression and enhances epithelial to mesenchymal transition of mammary epithelial cells: Potential involvement of ZEB-1 and ZEB-2. Oncogene 26: 711-724, 2007.
47. Medici D and Nawshad A: Type I collagen promotes epithelial-mesenchymal transition through ILK-dependent activation of NF-kappaB and LEF-1. Matrix Biol 29: 161-165, 2010.
48. Wang X, Belguise K, Kersual N, Kirsch KH, Mineva ND, Galtier F, Chalbos D and Sonenshein GE: Oestrogen signalling inhibits invasive phenotype by repressing RelB and its target BCL2. Nat Cell Biol 9: 470-478, 2007.
49. Sarkar FH, Li Y, Wang Z and Kong D: NF-kappaB signaling pathway and its therapeutic implications in human diseases. Int Rev Immunol 27: 293-319, 2008.
50. Huang CY, Lee CY, Chen MY, Yang WH, Chen YH, Chang CH, Hsu HC, Fong YC and Tang CH: Stromal cell-derived factor-1/CXCR4 enhanced motility of human osteosarcoma cells involves MEK1/2, ERK and NF-kappaB-dependent pathways. J Cell Physiol 221: 204-212, 2009.
51. Felx M, Guyot MC, Isler M, Turcotte RE, Doyon J, Khatib AM, Leclerc S, Moreau A and Moldovan F: Endothelin-1 (ET-1) promotes MMP-2 and MMP-9 induction involving the transcription factor NF-kappaB in human osteosarcoma. Clin Sci (Lond) 110: 645-654, 2006.
52. Iyer SV, Ranjan A, Elias HK, Parrales A, Sasaki H, Roy BC, Umar S, Tawfik OW and Iwakuma T: Genome-wide RNAi screening identifies TMIGD3 isoform1 as a suppressor of NF-κB and osteosarcoma progression. Nat Commun 7: 13561, 2016.
53. Zhou J, Liu Q, Qian R, Liu S, Hu W and Liu Z: Paeonol antagonizes oncogenesis of osteosarcoma by inhibiting the function of TLR4/MAPK/NF-κB pathway. Acta Histochem 122: 151455, 2020.
54. Yang M, Liu B, Jin L, Tao H and Yang Z: Estrogen receptor β exhibited anti-tumor effects on osteosarcoma cells by regulating integrin, IAP, NF-kB/BCL-2 and PI3K/Akt signal pathway. J Bone Oncol 9: 15-20, 2017.